Electronic Supplementary Material (ESI) for Journal of Materials Chemistry A.

Electronic Supplementary Information

Active Sites-enriched Hierarchical MoS_2 Nanotubes: Highly Active and Stable Architectures for Boosting Hydrogen Evolution and Lithium Storage

Jin Wang,[† ⊥ //] Jilei Liu,[# ⊥ //] Hao Yang,[‡*] Zhen Chen,[† ⊥] Jianyi Lin,[# *] and Ze Xiang Shen[†⊥*]

[†] *Energy Research Institute (ERI@N), Interdisciplinary Graduate School, Nanyang Technological University, Research Techno Plaza, 50 Nanyang Drive, 637553, Singapore*

[⊥] *Division of Physics and Applied Physics, School of Physical and Mathematical Sciences, Nanyang Technological University, 21 Nanyang Link, 637371, Singapore*

[#] *Energy Research Institute (ERI@N), Nanyang Technological University, 50 Nanyang Drive, 637553, Singapore*

[‡] *Jiangsu Key Laboratory of Advanced Laser Materials and Devices, School of Physics and Electronic Engineering, Jiangsu Normal University, Xuzhou 221116, China.*

[*] *E-mail: zexiang@ntu.edu.sg; Lijy@ntu.edu.sg; yanghao@jsnu.edu.cn*

[//] J. Wang and J. L. Liu contributed equally to this work.

Table S1 A survey of electrochemical properties of MoS_2 and its hybrid composites for LIBs.

Electrode description	**1st Specific capacity (mAhg^{-1})**	**1st Coulombic efficiency**	**Cycling stability**	**Rate performance**
MT@MS/GF (this work)	1487 mAh g^{-1} at 100 mA g^{-1}	81.7%	892 mAh g^{-1} after 200 cycles at 500 mA g^{-1}	1025, 916 and 775 mAh g^{-1} at 1000, 2000 and 5000 mA g^{-1}
Honeycomb-like MoS_2 nanoarchitectures on 3DGF [1]	1397 mAh g^{-1} at 100 mA g^{-1}	82.9%	1100 mAh g^{-1} after 60 cycles at 200 mA g^{-1}	1172, 1095, 1007, 966 and 800 mAh g^{-1} at 200, 500, 1000, 2000 and 5000 mA g^{-1}
Worm-like MoS_2 nanoarchitectures on GF/CNTs film[3]	1568 mAh g^{-1} at 100 mA g^{-1}	79.8%	1112 mAh g^{-1} after 120 cycles at 200 mA g^{-1}	1368, 1140, 1064, 1006 and 823 mAh g^{-1} at 200, 500, 1000, 2000 and 5000 mA g^{-1}
MoS_2@graphene nanocables [4]	1150 mAh g^{-1} at 500 mA g^{-1}		900 mAh g^{-1} after 700 cycles at 5 A g^{-1}	1150 and 700 mAh g^{-1} at 500 mA g^{-1} and 10 A g^{-1}
MoS_2-carbon nanofiber composite [5]	1712 mAh g^{-1} at 100 mA g^{-1}	74%	1007 mAh g^{-1} after 100 cycles at 1 A g^{-1}	1095, 986, 768, 637, 620, 548 and 347 mAh g^{-1} at 0.5, 1, 5, 10, 20, 30 and 50 A g^{-1}
MoS_2-graphene-carbon nanotube nanocomposites [6]	949 mAh g^{-1} at 100 mA g^{-1}		886 mAh g^{-1} after 100 cycles at 1 A g^{-1}	949, 883, 858, 737 and 652 mAh g^{-1} at 100, 500, 1000, 5000 and 10000 mA g^{-1}
Hierarchical C@MoS_2 microspheres [7]			750 mAh g^{-1} after 50 cycles at 100 mA g^{-1}	500 mAh g^{-1} at 1000 mA g^{-1}
MoS_2 nanoflake array/carbon cloth[8]	3.5 mAh cm^{-2} at a current density of 0.15 mA cm^{-2}	97.6%		3.26, 2.73, 2.39, 1.72, 1.24, and 0.85 mAh cm^{-2} at current densities of 0.15, 0.3, 0.75, 1.5, 2.25, and 3.0 mA cm^{-2}
MoS_2/3DGN[9]	1222 mAh g^{-1} at 100 mA g^{-1}	83.50%	877 mAh g^{-1} after 50 cycles	849, 782, 692, 597 and 466 mAh g^{-1} at

			at 100 mA g^{-1}	100, 200, 500, 1000 and 4000 mA g^{-1}
MoS_2/graphene nanosheet[10]	2200 mAh g^{-1} at 100 mA g^{-1}	59.10%	1290 mAh g^{-1} after 50 cycles at 100 mA g^{-1}	1040 mAh g^{-1} at 1000 mA g^{-1}
MoS_2/graphene composites[11]	1462 mAh g^{-1} at 100 mA g^{-1}	58.5%	1187 mAh g^{-1} after 100 cycles at 100 mA g^{-1}	900 mAh g^{-1} at 1000 mA g^{-1}
MoS_2/amorphous carbon[12]	2100 mAh g^{-1} at 100 mA g^{-1}	44.10%	912 mAh g^{-1} after 100 cycles at 100 mA g^{-1}	
CNT@MoS_2[13]	1434 mAh g^{-1} at 100 mA g^{-1}	60.01%	698 mAh g^{-1} after 60 cycles at 100 mA g^{-1}	653, 459 and 369 mAh g^{-1} at 200, 500 and 1000 mA g^{-1}
MoS_2/amorphous carbon[14]	2108 mAh g^{-1} at 100 mA g^{-1}	79%	755 mAh g^{-1} after 100 cycles at 100 mA g^{-1}	850 mAh g^{-1} at 400 mA g^{-1}
MoS_2/PS microspheres[15]	1160 mAh g^{-1} at 100 mA g^{-1}	68.20%	672 mAh g^{-1} after 50 cycles at 100 mA g^{-1}	726, 581 and 353 mAh g^{-1} at 200, 500 and 1000 mA g^{-1}
Graphene-network-backnoned MoS_2[16]	1200 mAh g^{-1} at 600 mA g^{-1}	68%	1200 mAh g^{-1} after 30 cycles at 600 mA g^{-1}	620 and 270 mAh g^{-1} at 7200 and 84000 mA g^{-1}
MoS_2 nanoplates[17]	1062 mAh g^{-1} at 1062 mA g^{-1}	87%	907 mAh g^{-1} after 50 cycles at 100 mA g^{-1}	790 and 700 mAh g^{-1} at 31.8 and 53.1A g^{-1}
3D MoS_2 flowers[18]	869 mAh g^{-1} at 100 mA g^{-1}	65.90%	633 mAh g^{-1} after 50 cycles at 100 mA g^{-1}	848 and 740 mAh g^{-1} at 100 and 400 mA g^{-1}
Mesoporous MoS_2[19]	1052 mAh g^{-1} at 100 mA g^{-1}	83.90%	876 mAh g^{-1} after 100 cycles at 100 mA g^{-1}	903, 880, 845, 795, 748, 670 and 608 mAh g^{-1} at 100, 200, 500, 1000, 2000 and 5000 mA g^{-1}
MoS_2/CNT network[20]	1715 mAh g^{-1} at 200 mA g^{-1}	76.10%	1456 mAh g^{-1} after 50 cycles at 200 mA g^{-1}	1431, 1367, 1302 and 1224 mAh g^{-1} at 400, 600, 800 and 1000 mA g^{-1}
MoS_x/CNT[21]	1549 mAh g^{-1} at 50 mA g^{-1}	74.80%	≥1000 mAh g^{-1} after 40 cycles	1119, 904, 659, 358 and 197 mAh

			at 50 mA g^{-1}	g^{-1} at 50, 200, 500 and 1000 mA g^{-1}
MoS_2-CNT film[22]	1117 mAh g^{-1} at 100 mA g^{-1}	73.40%	960 mAh g^{-1} after 100 cycles at 100 mA g^{-1}	670 (3200) 670 mAh g^{-1} at 3200 mA g^{-1}
Hollow MoS_2 nanoparticles[23]	1236 mAh g^{-1} at 100 mA g^{-1}	74%	902 mAh g^{-1} after 80 cycles at 100 mA g^{-1}	1030, 950, 910, 850 and 780 mAh g^{-1} at 100, 200, 300, 500 and 1000 mA g^{-1}
3D MoS_2 assembly tubes[24]	1172 mAh g^{-1} at 100 mA g^{-1}	68.30%	839 mAh g^{-1} after 50 cycles at 100 mA g^{-1}	600 and 500 mAh g^{-1} at 1000 and 5000 mA g^{-1}
MoS_2-graphene composites[25]	1367 mAh g^{-1} at 100 mA g^{-1}	66.70%	808 mAh g^{-1} after 100 cycles at 100 mA g^{-1}	571 mAh g^{-1} at 1000 mA g^{-1}
PEO/MoS_2/graphene [26]	1150 mAh g^{-1} at 50 mA g^{-1}	74%	≥1000 mAh g^{-1} after 180 cycles at 50 mA g^{-1}	650 mAh g^{-1} at 200 mA g^{-1}
MoS_2/polyaniline[27]	1460 mAh g^{-1} at 100 mA g^{-1}	72.80%	953 mAh g^{-1} after 50 cycles at 100 mA g^{-1}	1006 mAh g^{-1} at 200 mA g^{-1}
MoS_2/C nanotube[28]	1320 mAh g^{-1} at 200 mA g^{-1}	70.50%	776 mAh g^{-1} after 100 cycles at 200 mA g^{-1}	450-600 mAh g^{-1} at 1000 mA g^{-1}
MoS_2@carbon spheres[7]	1020 mAh g^{-1} at 100 mA g^{-1}	73.50%	750 mAh g^{-1} after 50 cycles at 100 mA g^{-1}	500 mAh g^{-1} at 1000 mA g^{-1}
MoS_2@carbon layer[29]	1251 mAh g^{-1} at 1000 mA g^{-1}	90.70%	814 mAh g^{-1} after 100 cycles at 1000 mA g^{-1}	600 mAh g^{-1} at 4000 mA g^{-1}
MoS_2@CMK-3[30]	1056 mAh g^{-1} at 250 mA g^{-1}	78.03%	602 mAh g^{-1} after 100 cycles at 250 mA g^{-1}	832, 774, 666 and 564 mAh g^{-1} at 250, 500, 1000 and 2000 mA g^{-1}
Fe_3O_4/MoS_2[31]	1320 mAh g^{-1} at 100 mA g^{-1}	81.74%	1200 mAh g^{-1} after 560 cycles at 500 mA g^{-1}	1189, 943, 569, 362 and 270, 224 mAh g^{-1} at 1000, 2000, 4000, 6000, 8000 and 10000 mA g^{-1}
MoS_2/TiO_2[32]	931 mAh g^{-1} at 100 mA g^{-1}	74%	472 mAh g^{-1} after 100 cycles at 100 mA g^{-1}	713, 636, 533 and 461 mAh g^{-1} at 100, 200, 500 and

	1000 mA g^{-1}

Table S2 A survey of electrochemical properties of MoS_2 and its hybrid composites for HER.

Catalyst	Tafle Slope [mV decade^{-1}]	Onset overpotential [mV vs RHE]	Exchange current densities (j_0) [mA cm^{-2}]
MT@MS/GF (this work)	52	77	6.4*10^{-2}
Defect-rich MoS_2 nanosheets [32]	50	120	8.91*10^{-3}
MoS_2/$CoSe_2$ hybrids [33]	36	11	7.3*10^{-2}
graphene-surpported MoS_2[34]	41	~100	
MoS_x Grown on Graphene-Protected 3D Ni Foams[35]	42.8	109-141	
MoO_3–MoS_2 Nanowires[36]	50-60	150-200	
MoS_2 on Mesoporous Graphene[37]	42	90-120	
MoS_2 nanofilms[38]	43~47	113	0.13~0.25
MoS_2/N-doped CNT[39]	40	~75	3.3*10^{-2}
MoS_2 nanoflower/rGO paper[40]	95	190	
MoS_2 on 3D substrates[41]	62	~100	
Mesoporous MoS_2[42]	50	150-200	

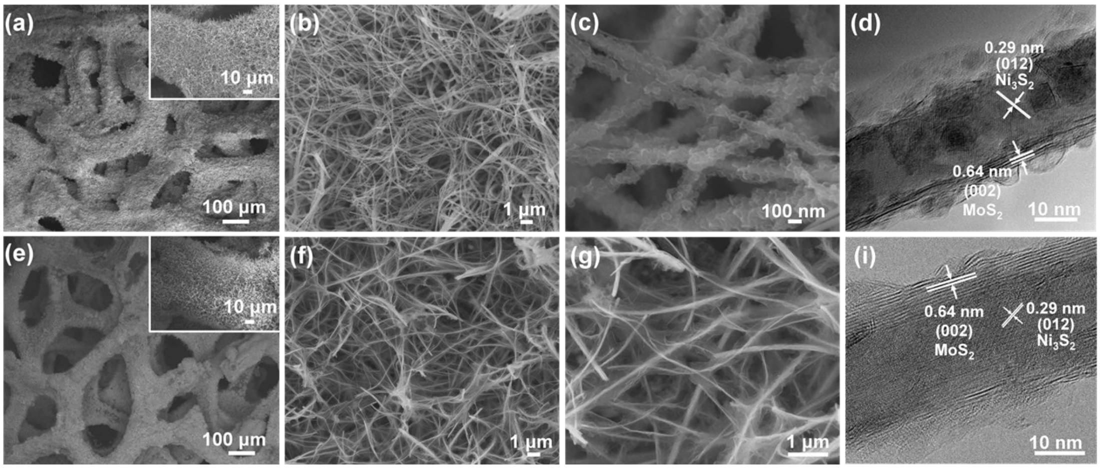

Figure S1. SEM and TEM images of (a-d) $MoS_2/Ni_3S_2@MoS_2$ and (e-i) $Ni_3S_2@MoS_2$.

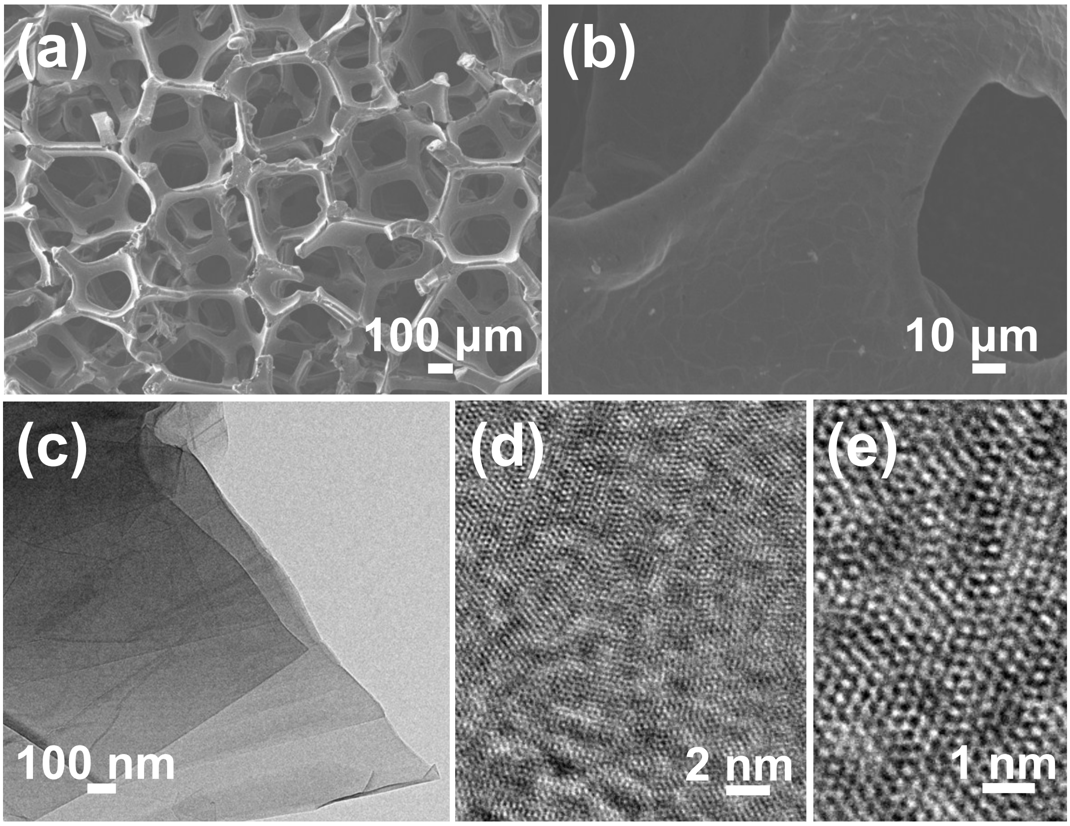

Figure S2. SEM (a-b), and TEM (c-e) images of GF.

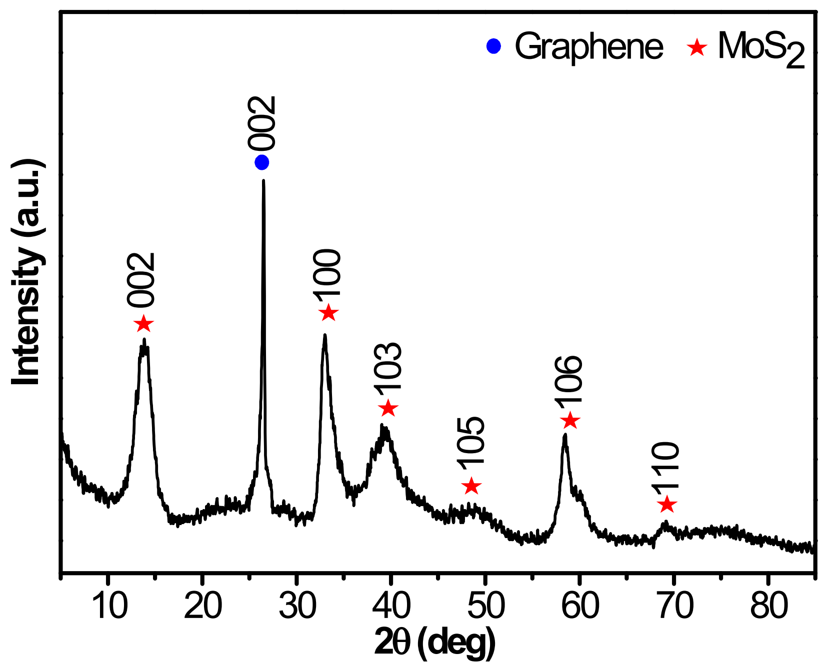

Figure S3 XRD pattern of MT/GF.

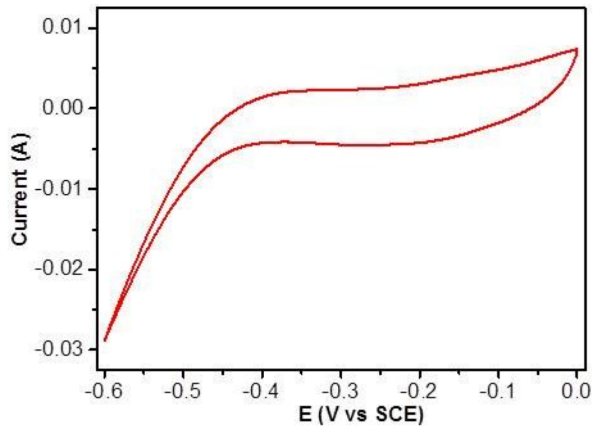

Figure S4. Cyclic voltammograms of the MT@MS/GF recorded between -0.6 and 0 V (*vs.* SCE, in 0.5 M H_2SO_4) at a sweep rate of 5 mV s^{-1}.

Explanation of the calculation of catalytic parameters:

(a) All the parameters were measured under the same conditions, i.e., the MT@MS/GF and MT/GF catalyst with loading weights of 1.2 and 0.5 mg cm^{-2} on GF directly tested in 0.5 M H_2SO_4 solution;

(b) Calculation of active sites;

The absolute components of voltammetric charges which include both the cathodic and anodic scans can be attained from the CV shown in the **Figure S3**. The total absolute charge is then divided by two, assuming a one electron redox process. Later, this value is further divided by Faraday constant to get number of active sites (in moles) of the MT@MS /GF and MT/GF.

(c) TOFs were measured at η = 300 mV;

Once the number of active sites is obtained, the turn over frequency (TOF) can be calculated using the equation:

$$TOF = \frac{I\ 1}{Fn2}$$

Where,

I – Current in Amperes during the linear sweep measurement.

F – Faraday constant in C/mol.

n – Number of active sites in mol. The factor ½ represents that 2 electrons are required to form one hydrogen molecule from two protons.

(d) Exchange current densities (j_0) were obtained from Tafel curves by using extrapolation methods.

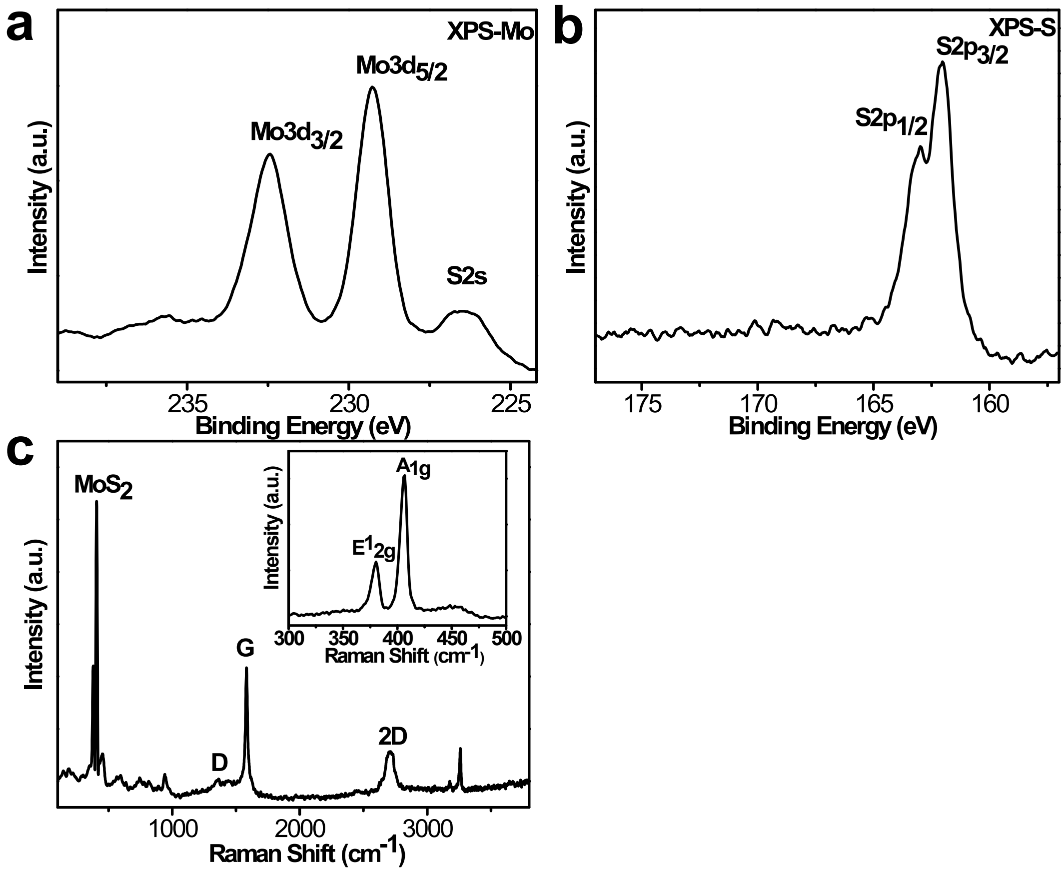

Figure S5. Detailed microstructure characterization after long-term HER cycling test. XPS spectra of (a) Mo 3d peaks and (b) S 2p peaks of the MT@MS/GF. (c) Raman spectra of the MT@MS/GF.

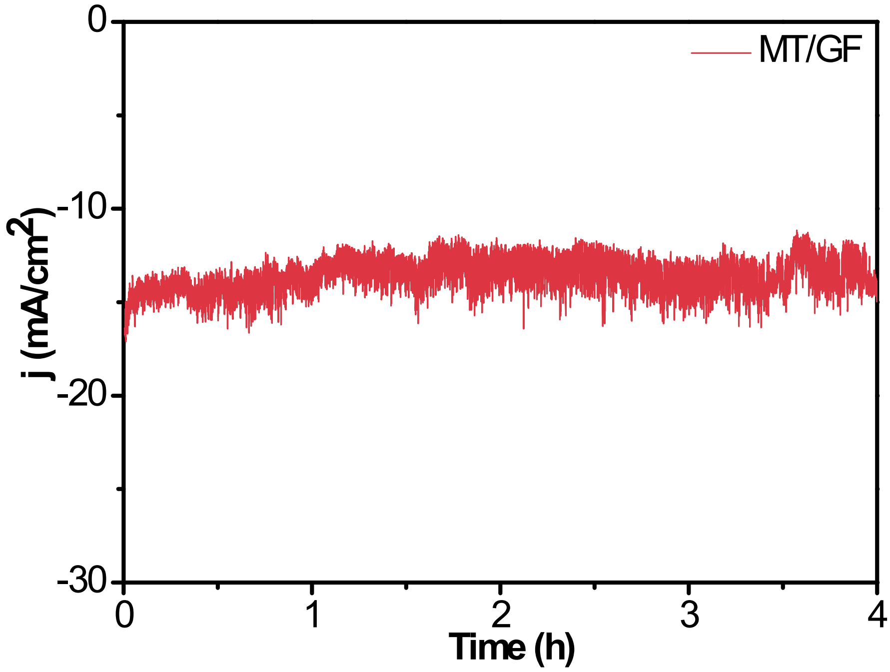

Figure S6. Time dependence of current density for the MT/GF catalyst under a constant potential of –0.17 V vs RHE.

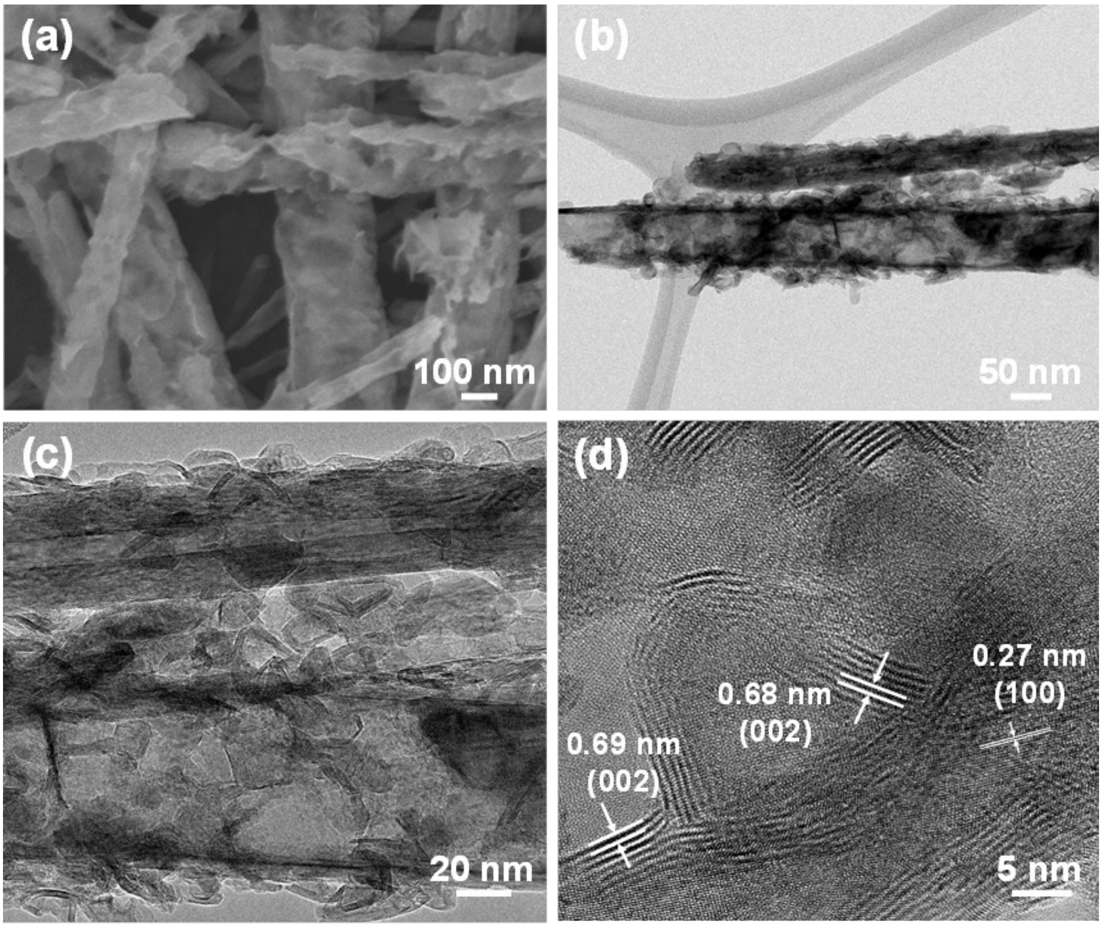

Figure S7. Detailed morphology characterization after long-term HER cycling test. a) SEM images of MT@MS. b) TEM image of MT@MS. c, d) HRTEM images of MT@MS, showing MoS_2 nanosheets decorating MoS_2 nanotubes and crystal planes of MT@MS.

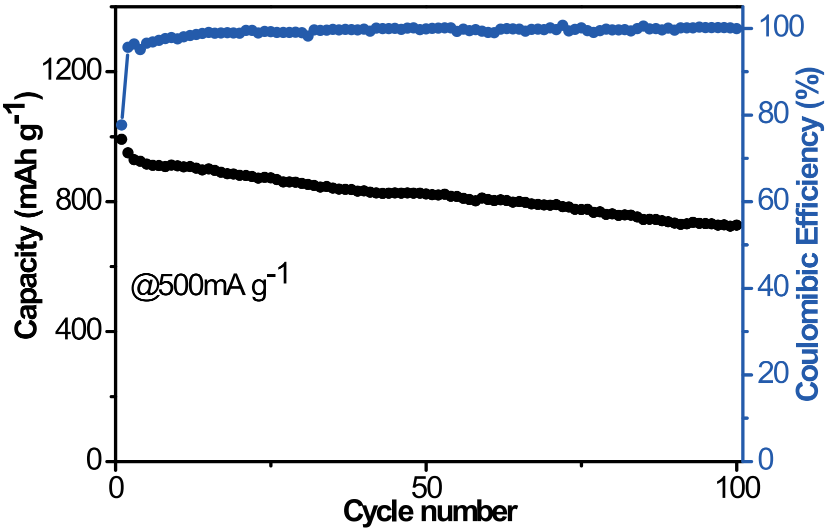

Figure S8 Cycling behaviors of the MT@MS/GF electrode at a current density of 500 mA g^{-1}.

Table S3 The comparison of electrochemical performances for two electrodes, MT@MS/GF and MT/GF.

Electrode description	1st Specific capacity (mAhg^{-1})	1st Coulombic efficiency	Cycling stability (%)	Rate performance
MT@MS/GF	1487 mAh g^{-1} at 100 mA g^{-1}	81.7%	892 mAh g^{-1} after 200 cycles at 500 mA g^{-1}	1025, 916 and 775 mAh g^{-1} at 1000, 2000 and 5000 mA g^{-1}
MT/GF	1382 mAh g^{-1} at 100 mA g^{-1}	75.2%	727 mAh g^{-1} after 100 cycles at 500 mA g^{-1}	894, 765 and 648 mAh g^{-1} at 1000, 2000 and 5000 mA g^{-1}

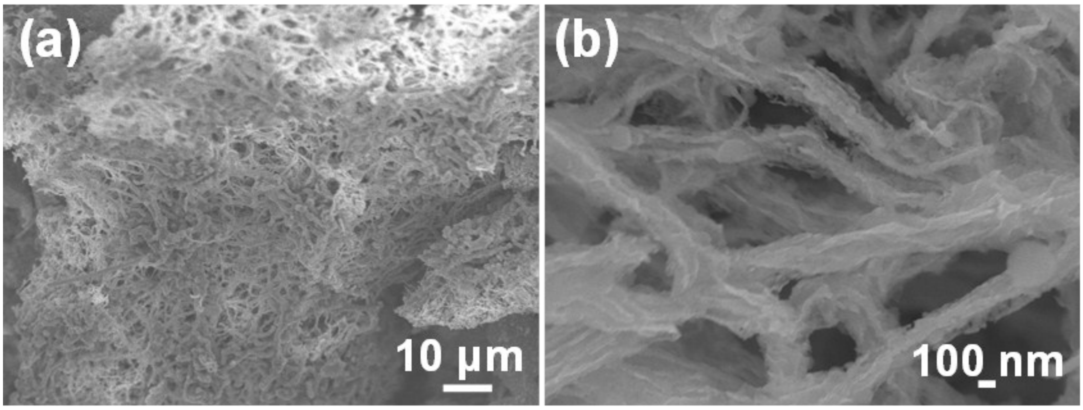

Figure S9. SEM images of the MT@MS/GF electrode as anode of LIBs after cycling for 200 times at a current density of 500 mA g^{-1}.

Reference

1. Wang, J.; Liu, J.; Chao, D.; Yan, J.; Lin, J.; Shen, Z. X., *Adv Mater* **2014,** *26* (42), 7162-9.
3. Kong, D. B.; He, H. Y.; Song, Q.; Wang, B.; Lv, W.; Yang, Q. H.; Zhi, L. J., *Energy & Environmental Science* **2014,** *7* (10), 3320-3325.
4. Zhu, C.; Mu, X.; van Aken, P. A.; Yu, Y.; Maier, J., *Angewandte Chemie International Edition* **2014,** *53* (8), 2152-2156.
5. Zhu, C. B.; Mu, X. K.; van Aken, P. A.; Maier, J.; Yu, Y., *Advanced Energy Materials* **2015,** *5* (4), Doi: 10.1002/Aenm.201401170.
6. Zhang, L.; Lou, X. W., *Chemistry – A European Journal* **2014,** *20* (18), 5219-5223.
7. Yu, H.; Zhu, C.; Zhang, K.; Chen, Y.; Li, C.; Gao, P.; Yang, P.; Ouyang, Q., *Journal of Materials Chemistry A* **2014,** *2* (13), 4551-4557.
8. Cao, X.; Shi, Y.; Shi, W.; Rui, X.; Yan, Q.; Kong, J.; Zhang, H., *Small* **2013,** *9* (20), 3433-3438.
9. Chang, K.; Chen, W., *Chemical Communications* **2011,** *47* (14), 4252-4254.
10. Chang, K.; Chen, W., *ACS Nano* **2011,** *5* (6), 4720-4728.
11. Chang, K.; Chen, W.; Ma, L.; Li, H.; Li, H.; Huang, F.; Xu, Z.; Zhang, Q.; Lee, J.-Y., *Journal of Materials Chemistry* **2011,** *21* (17), 6251-6257.
12. Ding, S.; Chen, J. S.; Lou, X. W., *Chemistry – A European Journal* **2011,** *17* (47), 13142-13145.
13. Das, S. K.; Mallavajula, R.; Jayaprakash, N.; Archer, L. A., *Journal of Materials Chemistry* **2012,** *22* (26), 12988-12992.
14. Ding, S.; Zhang, D.; Chen, J. S.; Lou, X. W., *Nanoscale* **2012,** *4* (1), 95-98.
15. Gong, Y.; Yang, S.; Liu, Z.; Ma, L.; Vajtai, R.; Ajayan, P. M., *Advanced Materials* **2013,** *25* (29), 3979-3984.
16. Hwang, H.; Kim, H.; Cho, J., *Nano Letters* **2011,** *11* (11), 4826-4830.
17. Li, H.; Li, W.; Ma, L.; Chen, W.; Wang, J., *Journal of Alloys and Compounds* **2009,** *471* (1–2), 442-447.
18. Liu, H.; Su, D.; Zhou, R.; Sun, B.; Wang, G.; Qiao, S. Z., *Advanced Energy Materials* **2012,** *2* (8), 970-975.
19. Lu, C.; Liu, W.-w.; Li, H.; Tay, B. K., *Chemical Communications* **2014**.
20. Shi, Y.; Wang, Y.; Wong, J. I.; Tan, A. Y. S.; Hsu, C.-L.; Li, L.-J.; Lu, Y.-C.; Yang, H. Y., *Sci. Rep.* **2013,** *3*.
21. Wang, J.-Z.; Lu, L.; Lotya, M.; Coleman, J. N.; Chou, S.-L.; Liu, H.-K.; Minett, A. I.; Chen, J., *Advanced Energy Materials* **2013,** *3* (6), 798-805.
22. Wang, M.; Li, G.; Xu, H.; Qian, Y.; Yang, J., *ACS Appl Mater Interfaces* **2013,** *5* (3), 1003-8.
23. Wang, P. P.; Sun, H.; Ji, Y.; Li, W.; Wang, X., *Adv Mater* **2014,** *26* (6), 964-9.
24. Wang, Z.; Chen, T.; Chen, W.; Chang, K.; Ma, L.; Huang, G.; Chen, D.; Lee, J. Y., *Journal of Materials Chemistry A* **2013,** *1* (6), 2202-2210.
25. Xiao, J.; Wang, X. J.; Yang, X. Q.; Xun, S. D.; Liu, G.; Koech, P. K.; Liu, J.; Lemmon, J. P., *Advanced Functional Materials* **2011,** *21* (15), 2840-2846.
26. Yang, L.; Wang, S.; Mao, J.; Deng, J.; Gao, Q.; Tang, Y.; Schmidt, O. G., *Advanced Materials* **2013,** *25* (8), 1180-1184.
27. Zhang, C.; Wang, Z.; Guo, Z.; Lou, X. W., *ACS Applied Materials & Interfaces* **2012,** *4* (7), 3765-3768.
28. Zhao, X.; Hu, C.; Cao, M., *Chemistry – An Asian Journal* **2013,** *8* (11), 2701-2707.
29. Zhou, X. S.; Wan, L. J.; Guo, Y. G., *Nanoscale* **2012,** *4* (19), 5868-5871.

30. Chen, Y.; Song, B.; Tang, X.; Lu, L.; Xue, J., *Small* **2014,** *10* (8), 1536-1543.
31. Xu, X.; Fan, Z.; Ding, S.; Yu, D.; Du, Y., *Nanoscale* **2014,** *6* (10), 5245-5250.
32. Xie, J.; Zhang, H.; Li, S.; Wang, R.; Sun, X.; Zhou, M.; Zhou, J.; Lou, X. W.; Xie, Y., *Advanced Materials* **2013,** *25* (40), 5807-5813.
33. Gao, M. R.; Liang, J. X.; Zheng, Y. R.; Xu, Y. F.; Jiang, J.; Gao, Q.; Li, J.; Yu, S. H., *Nat Commun* **2015,** *6*, 5982.
34. Li, Y.; Wang, H.; Xie, L.; Liang, Y.; Hong, G.; Dai, H., *Journal of the American Chemical Society* **2011,** *133* (19), 7296-7299.
35. Chang, Y.-H.; Lin, C.-T.; Chen, T.-Y.; Hsu, C.-L.; Lee, Y.-H.; Zhang, W.; Wei, K.-H.; Li, L.-J., *Advanced Materials* **2013,** *25* (5), 756-760.
36. Chen, Z.; Cummins, D.; Reinecke, B. N.; Clark, E.; Sunkara, M. K.; Jaramillo, T. F., *Nano Letters* **2011,** *11* (10), 4168-4175.
37. Liao, L.; Zhu, J.; Bian, X.; Zhu, L.; Scanlon, M. D.; Girault, H. H.; Liu, B., *Advanced Functional Materials* **2013,** *23* (42), 5326-5333.
38. Wang, H.; Lu, Z.; Xu, S.; Kong, D.; Cha, J. J.; Zheng, G.; Hsu, P.-C.; Yan, K.; Bradshaw, D.; Prinz, F. B.; Cui, Y., *Proceedings of the National Academy of Sciences* **2013,** *110* (49), 19701-19706.
39. Li, D. J.; Maiti, U. N.; Lim, J.; Choi, D. S.; Lee, W. J.; Oh, Y.; Lee, G. Y.; Kim, S. O., *Nano Letters* **2014,** *14* (3), 1228-1233.
40. Ma, C.-B.; Qi, X.; Chen, B.; Bao, S.; Yin, Z.; Wu, X.-J.; Luo, Z.; Wei, J.; Zhang, H.-L.; Zhang, H., *Nanoscale* **2014,** *6* (11), 5624-5629.
41. Wang, H.; Lu, Z.; Kong, D.; Sun, J.; Hymel, T. M.; Cui, Y., *ACS Nano* **2014,** *8* (5), 4940-4947.
42. Kibsgaard, J.; Chen, Z.; Reinecke, B. N.; Jaramillo, T. F., *Nat Mater* **2012,** *11* (11), 963-969.